

Review

Mechanistic Insights into Graphene Oxide Driven Photocatalysis as Co-Catalyst and Sole Catalyst in Degradation of Organic Dye Pollutants

Jai Prakash 

Department of Chemistry, National Institute of Technology Hamirpur,
Hamirpur 177005, Himachal Pradesh, India; jaip@nith.ac.in; Tel.: +91-991-053-3582

Abstract: Photocatalysis is a promising route to utilize sunlight, which has been potentially used to solve energy as well as environmental problems with an emphasis on fundamental understanding and technological applications in society. Semiconductors are excellent photocatalysts but often show less efficient activities due to the fast recombination of photogenerated charge carriers and very slow kinetics of surface photochemical reactions. However, recent advancements show promising strategies to improve their photocatalytic activities, including surface modifications using suitable co-catalysts and the development of novel efficient photocatalysts. Graphene oxide (GO) is one of such nanomaterials which shows multifarious roles in photocatalysis with a great potential to act as an independent solar-driven sole photocatalyst. In this minireview, the photochemistry of GO has been discussed in view of its multifarious roles/mechanisms in improving the photocatalytic activity of metal oxide semiconductors, plasmonic nanomaterials, and also their nanocomposites. In addition, recent advancements and applications of such GO-based photocatalysts in photocatalytic degradation of organic dye pollutants, including engineering of GO as the sole photocatalyst, have been discussed. Furthermore, the challenges and future prospects for the development of GO-based photocatalysts are discussed.



Citation: Prakash, J. Mechanistic Insights into Graphene Oxide Driven Photocatalysis as Co-Catalyst and Sole Catalyst in Degradation of Organic Dye Pollutants. *Photochem* **2022**, *2*, 651–671. <https://doi.org/10.3390/photochem2030043>

Academic Editor: Vincenzo Vaiano

Received: 9 July 2022

Accepted: 15 August 2022

Published: 17 August 2022

Publisher's Note: MDPI stays neutral with regard to jurisdictional claims in published maps and institutional affiliations.



Copyright: © 2022 by the author. Licensee MDPI, Basel, Switzerland. This article is an open access article distributed under the terms and conditions of the Creative Commons Attribution (CC BY) license (<https://creativecommons.org/licenses/by/4.0/>).

Keywords: graphene oxide; co-catalysts; sole catalysts; photocatalysis; mechanisms; dye pollutants

1. Introduction

In recent years, several sustainable nanomaterials and techniques for water treatment have been extensively studied and are shown to be capable of improving the quality of water [1–5]. However, photocatalyst nanomaterials capable of solar-to-chemical energy conversion through photocatalytic technology have gained great attention due to their low-cost processing, environmentally friendly nature, and potential to solve the energy crisis as well as environmental pollution issues [6,7]. In this regard, several sole and composite photocatalysts, including metal oxide semiconductors, noble metals, other semiconductors, and their hybrid nanocomposite photocatalysts, have been investigated for various photocatalytic processes in energy and environmental applications [8–14]. However, with the continuous development of photocatalytic technology in a wide range of energy and environmental applications, it has been realized that there are still several challenges to industrializing this technology for practical applications on a large scale [4,9,11,15]. The major challenge is to produce photocatalyst nanomaterials with high photocatalytic efficiency, large specific area, and capable of absorbing a wide region of the solar spectrum. Furthermore, developing recyclable photocatalyst nanomaterials is another important aspect for long-term practical applications [16,17].

Recent developments in nanoscience and nanotechnology, along with the fundamental understanding of the coupling of nanomaterials, show that the surface modification of traditional metal oxide semiconductor photocatalysts using multifunctional co-catalysts would be a promising technique to overcome these challenges. Graphene oxide (GO) is

one of such nanomaterials which shows multifarious roles in photocatalysis and various important properties that can enhance the photocatalytic activities of other semiconductor photocatalysts, as shown in Figure 1 [14]. This is attributed to the unique structure and surface chemistry of GO, and it has been extensively used to modify metal oxide semiconductor photocatalysts due to its exceptional physiochemical properties [6,14,18], as discussed in the next section. Furthermore, GO, with an appropriate degree of oxidation, can be directly used as a photocatalyst for various redox reactions [9,14].

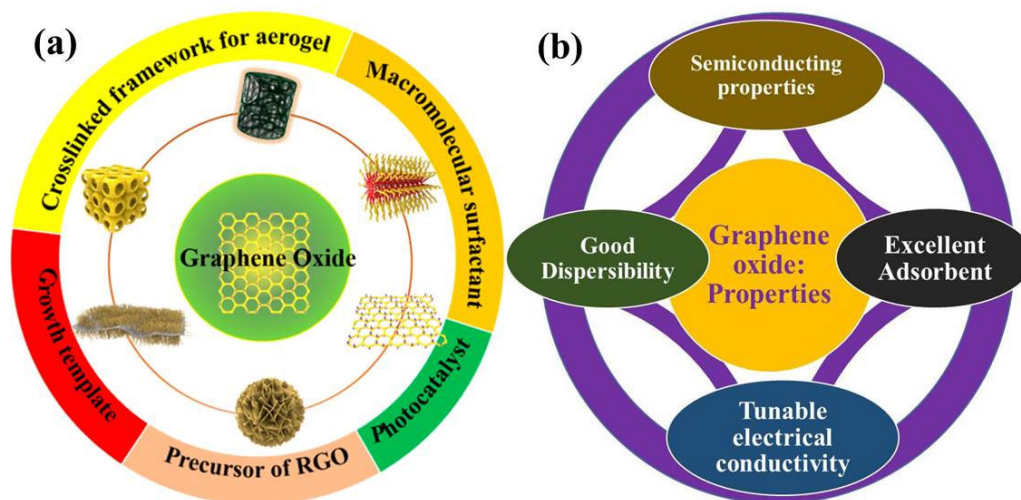


Figure 1. Schematic (a) multifarious roles [14] and (b) important properties GO in photocatalysis [14].

In this minireview, the photochemistry of GO has been discussed in view of its multifarious roles/mechanisms in improving photocatalytic activity of metal oxide semiconductors, plasmonic nanomaterials, and their nanocomposites as a co-catalyst. In addition, recent advancements and applications of such GO-based photocatalysts in photocatalytic degradation of organic pollutants, including engineering of GO as the sole photocatalyst, have been discussed. Furthermore, the challenges and future prospects for the development of GO-based photocatalysts are discussed, followed by a summary and conclusion.

2. Graphene Oxide: Surface Chemistry/Properties Related to Photocatalysis

Graphene and its derivatives, i.e., GO and reduced GO (rGO), have been studied in many research fields due to their unique properties. However, these nanostructures are different in many aspects. Figure 2a presents the chemical structures and electronic band diagrams of graphene, GO, and rGO. Graphene is a 2D-sheet-like hexagonal structure containing carbon atoms closely bonded to each atom with covalent bonds resulting in sp^2 -hybridization [9,19,20]. Due to the presence of π bonding with free electrons, it shows a highly conducting nature, but due to the hydrophobic sp^2 domain, graphene is not suitable for the photocatalytic process [21].

In the last few years, a great deal of research has been conducted on GO-based photocatalyst nanomaterials, and it has been considered one of the emerging photocatalysts [21]. GO is a type of oxidized graphene. As compared to graphene, GO has several changes in its structure resulting from the addition of oxygen-based functional groups, i.e., carboxylic, O-H, epoxy groups, etc. It shows hydrophilicity in water due to the presence of these polar groups that facilitate bond formation with water molecules. It is less conducting as compared to graphene, attributed to the structural disorder imposed by the sp^3 C-O bonds. However, it contributes to its dispersible nature attributed to the structure consisting of the sp^3 domain with hydrophilic oxygen-based functional groups [9,21]. In this way, GO possesses two regions, i.e., hydrophobic π -conjugated sp^2 domains and the sp^3 domains with hydrophilic oxygen-based various functional groups [22]. Furthermore, the valence band (VB) origin gradually shifts from π -orbital of graphene to oxygen 2p-orbital, whereas

the conduction band (CB) edge remains as π^* -orbital [21,23]. All these characteristics let GO a promising material with improved properties for potential applications in many research fields, including photocatalysis, as shown in Figure 2b [9,24,25]. It has an average band gap of 2.2 to 4 eV, making it a semiconductor with a fluctuation from the ultraviolet (UV)-to the visible region [25]. This property provides a base for its potential applications as a photocatalyst, which can be tuned by introducing an appropriate oxidation level.

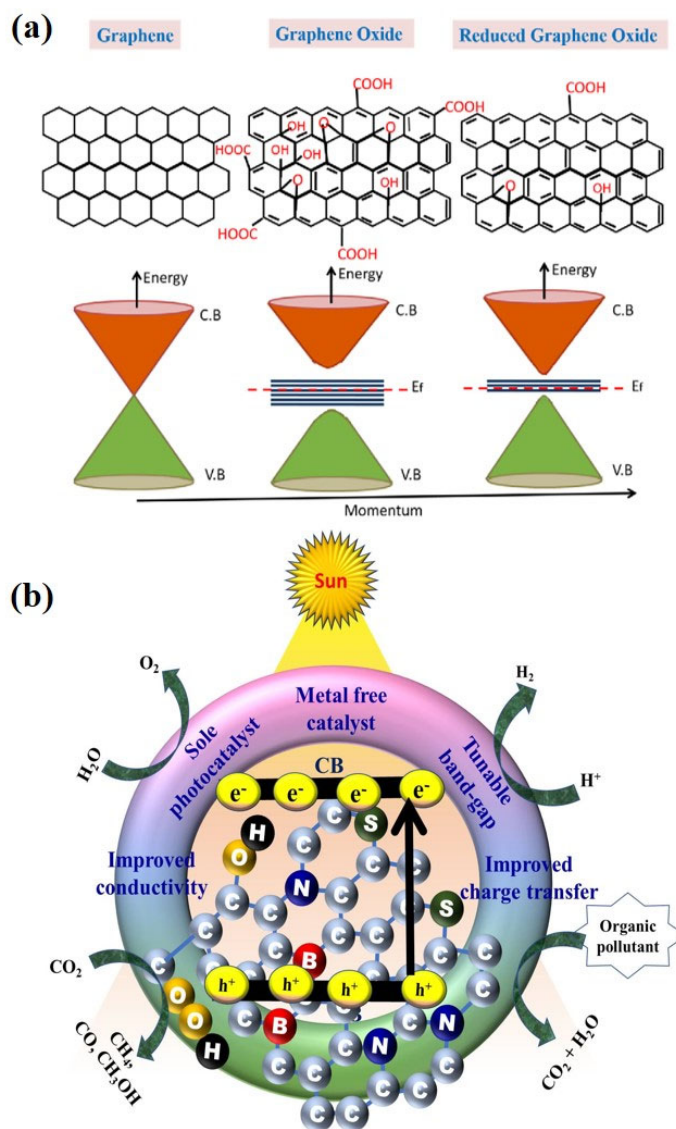


Figure 2. Schematic representation of: (a) Lattice structure and corresponding energy band diagrams of graphene, GO and rGO [26] (b) Multifunctional photocatalytic applications of GO in photocatalytic degradation, photocatalytic hydrogen production and photocatalytic CO₂ reduction induced by chemical doping in GO/rGO nanostructures [9].

Graphene structure is defect-free [19,20,27], whereas GO's structure is flawed due to the addition of different functional groups, resulting in varied electrical and thermal conductivities, specific surface areas, hydrophilicity, and hydrophobicity. When GO is reduced and the number of functional groups is decreased, i.e., rGO, the material behaves similar to graphene but is not entirely graphene due to the existence of some functional groups in its crystal structure [28–30]. rGO, as the modified form of GO, shows the greater surface area as optoelectronic properties along with adjustable bandgap attributed to the addition or deficiency of defects and oxygen groups [9,22]. Therefore, it is found that GO has more potential to be tuned for functional applications. It has also been reported that

GO can further be modified to enhance its photocatalytic activity by doping for different applications, as shown in Figure 2b, as discussed in the literature [9]. The doping of GO nanostructure allows control of the n- or p-type of character, charge transfer properties along with tailoring of its band gap and eventually convert into rGO [9,21,31,32]. Therefore, the study of both GO and rGO is important to understand the mechanism of photocatalytic action of GO.

3. Mechanistic Insights into Graphene Oxide Driven Photocatalysis in Degradation of Organic Dye Pollutants

3.1. Graphene Oxide as a Co-Catalyst

Metal oxide semiconductors such as TiO_2 , ZnO , etc., are the most used photocatalysts for different photocatalytic applications in the field of energy, environment, and biomedical [33–39]. These are wide band gap photocatalysts and absorb only UV radiation. Furthermore, these photocatalysts exhibit a high recombination rate of the photogenerated charge carriers. These photocatalysts have been modified in several ways to narrow their bandgap and suppress the charge recombination [6,8,10–12,16,40,41]. Particularly, GO, when combined with these semiconductor photocatalysts forming nanocomposites, prevents the recombination of photogenerated charge carriers separating photogenerated electrons and holes [9,42]. This is attributed to the unique structure of GO, which is easily hybridized with these photocatalysts providing a path for the separation/migration of electrons [43]. In addition, due to the presence of the unpaired pi-electrons in the GO structure as discussed above, it forms M-O-C bonds (Where, M = Ti, Zn, etc.) with metal oxide semiconductor photocatalysts which further improve their visible light absorption properties by band gap narrowing of the metal oxide semiconductors [24,44,45]. Figure 3a shows schematics of how oxygenated functional groups on GO form covalent bonds with TiO_2 semiconductor photocatalyst that eventually affects its electronic band structure by introducing a localized state within the bandgap [24,44]. This leads to the band gap narrowing of TiO_2 photocatalysts with enhanced visible light activity.

The various functional groups (i.e., unpaired pi-electrons) present in the GO sheet facilitate and mediate the efficient and uniform assembly of the metal oxide nanoparticles (NPs) onto the GO sheets leading to the excellent UV visible active nanocomposite photocatalysts [45–47]. Furthermore, in the case of photocatalytic degradation of organic dye molecules using GO-metal oxide semiconductor nanocomposites, GO nanomaterials play a promising role in enhancing the photocatalytic efficiency of the nanocomposites by strong adsorption of dye molecules [9,48]. Nguyen-Phan et al. [49] studied the role of GO as an adsorbent, electron transporter, and photosensitizer to enhance the photocatalytic activity of TiO_2 in the photodegradation of dye molecules. Figure 3b shows the absorption spectra of GO, TiO_2 , and GO- TiO_2 nanocomposites, demonstrating the role of GO in narrowing the band gap of TiO_2 with increasing GO content. Figure 3c,d show the FT-IR spectra of GO, TiO_2 , and GO- TiO_2 nanocomposites. It exhibits the formation of a Ti-O-C bond because of the strong coupling between GO and TiO_2 leading to the strong chemical interaction through the chemical bond formation. It was explained on the basis of shifting of the strong absorption bands in the range of $400\text{--}1000\text{ cm}^{-1}$ toward the lower region after incorporation of GO [49].

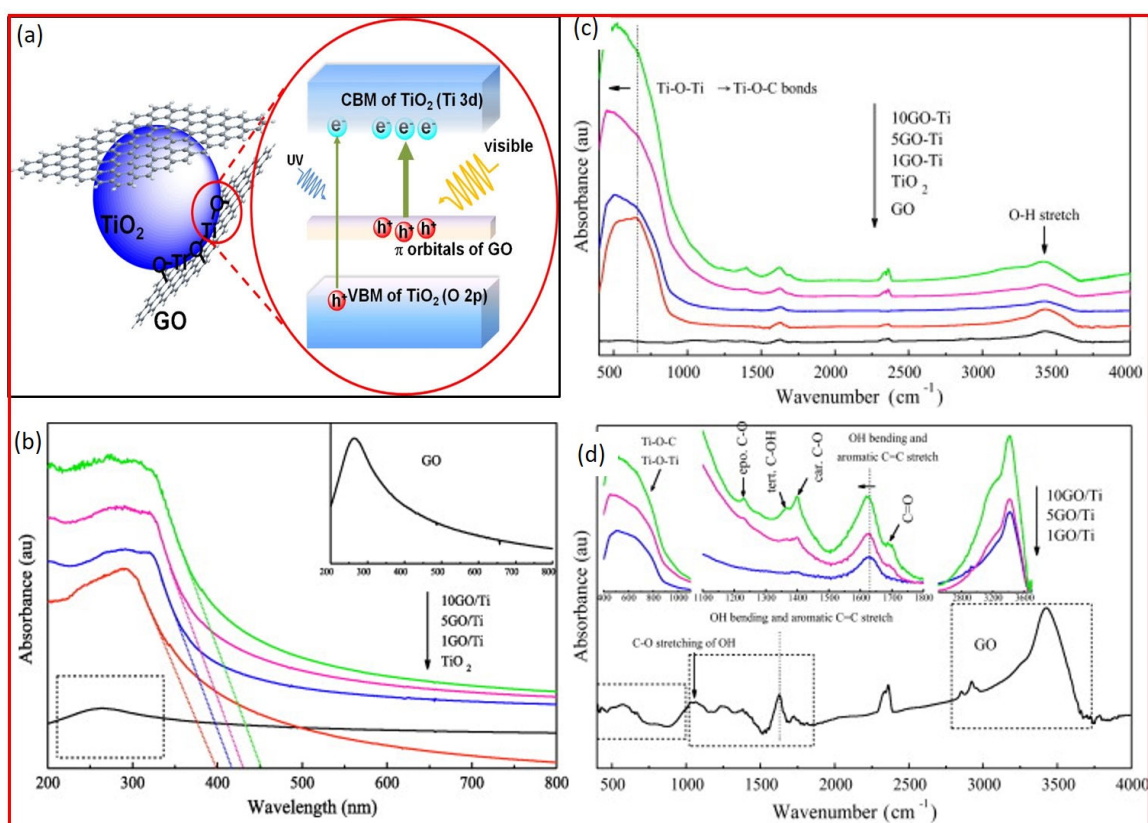


Figure 3. (a) Schematic shows Ti–O–C chemical bonding in GO–TiO₂ nanocomposites where GO introduces localized state within the band gap of TiO₂ through formation of covalent bond with TiO₂ [44]. (b) Absorption spectra of GO, TiO₂ and GO–TiO₂ nanocomposites. (c) Full FT-IR spectra and (d) selected/zoomed spectra from (c). Reprinted with permission from Ref. [49]. Copyright 2011-Elsevier.

Recently, Shaheen et al. [45] demonstrated that GO-doped ZnO exhibited excellent photocatalytic activities attributed to the narrowing of the band gap of GO–ZnO nanocomposites. This narrowing of the band gap was explained by the fact that GO acted as the photoexcited electron acceptor from the CB of ZnO, which migrated through the functional group, i.e., carboxyl groups on the GO–ZnO interface. This assembly provided an efficient path by shortening the electron transport path to GO. Victor-Roman et al. [47] demonstrated that surface chemistry of GO resulting from oxygenated functional groups played an important role in interface coupling for establishing interface interactions with ZnO leading to enhanced photocatalytic activities. They demonstrated that controlling the surface chemistry of GO through oxidation and GO loading with ZnO could be a promising way to tailor the photocatalytic properties of GO–ZnO nanocomposite. It was proposed that the control of the oxidation degree and optimization of the loading fraction of GO could be used to align the energy levels in nanocomposites resulting in the photoinduced electron transfer from CB of ZnO to lower energy states of GO under the exposure of the UV light (Figure 4a–d). It was attributed to the reduced recombination rate of photogenerated charge carriers resulting in the enhanced photocatalytic activity.

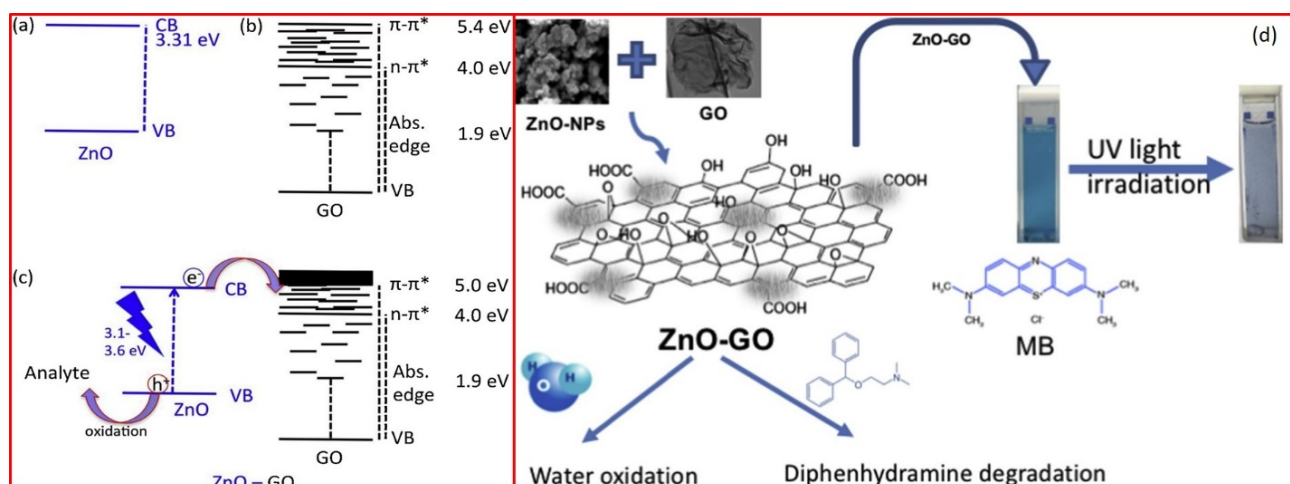


Figure 4. Schematic representation of energy levels of (a) ZnO, (b) GO and (c) ZnO–GO nanocomposites including VB, CB, absorption edge, $n-\pi^*$ and $\pi-\pi^*$ levels. (d) Schematic of GO–ZnO nanocomposite, interface interaction and degradation of MB dye molecules. Reprinted with permission from Ref. [47]. Copyright 2020-Elsevier.

Lin et al. [48] synthesized ZnO–GO nanocomposites and demonstrated that various oxygenated functional groups on GO served as anchor sites for the growth of ZnO nanocrystals resulting in flake-like composites nanostructures. Furthermore, it was concluded that enhanced photocatalytic activities of such nanocomposites as compared to the bare ZnO were attributed to the synergetic effect of ZnO and the role of GO as a catalysis carrier. Similarly, incorporating GO with ZnO led to the formation of ZnO–GO nanocomposite with reduced band gap and enhanced photocatalytic activity as compared to the ZnO [50]. Puneetha et al. [50] synthesized nanohybrid composites of GO–ZnO with an energy band gap of 2.71 eV, which demonstrated higher photocatalytic activity with 99% photodegradation and rate constant found to be 0.01514 min^{-1} of crystal violet (CV) using visible-light-induced photodegradation. The GO–ZnO nanohybrid showed better electron transport properties due to the incorporation of GO along with reduced charge recombination of photogenerated charge carriers.

The general mechanism of GO as charge carrier or electron transport/migration in GO-metal oxide nanocomposite can be described as shown in schematics of Figure 5a along with the reactions shown therein. Under the influence of visible light, when the GO-metal oxide photocatalyst becomes excited, first photogenerated electrons are excited from the VB of the metal oxide semiconductor to its CB. Here, GO acts as an electron trap, and these photoexcited electrons are transported to GO inhibiting their recombination with photogenerated holes in the VB. These electrons transported by GO then react with the surface oxygen leading to the production of reactive oxygen species (ROS), i.e., (O_2) radicals. On the other hand, the photogenerated holes in VB of metal oxide semiconductors react with water molecules to form other ROS, i.e., hydroxyl ($\cdot\text{OH}$) radicals. These radicals then degrade the dye molecules adsorbed on the surface of nanocomposite photocatalysts [51]. Another mechanism of enhanced photocatalytic dye degradation activity of GO-metal-oxide-based nanocomposites could be explained on the basis of effective charge transfer by GO from dye molecules to metal oxide photocatalysts [52,53]. Tien et al. [52] proposed that along with narrowing band gap of metal oxide semiconductor due to GO, dye induced visible light absorption and effective charge transfer by the adjusted energy levels among the dye molecule (i.e., MB). rGO and ZnO could be another possibility for the enhanced photocatalytic activity, as shown in the schematic of Figure 5b, along with the general chemical reaction mechanisms involved in effective charge transfer by GO. It was proposed that due to the large surface area of GO, dye molecules could be adsorbed on the surface of GO. If the dye molecules absorb the visible light radiation, then electrons from excited dye

molecules can be transferred to CB of the metal oxide through GO. In some cases, GO has been reported just as a better adsorbate for the dye molecules due to its large surface area, which plays an important role in enhancing the photocatalytic performance of metal oxide semiconductor photocatalysts [54].

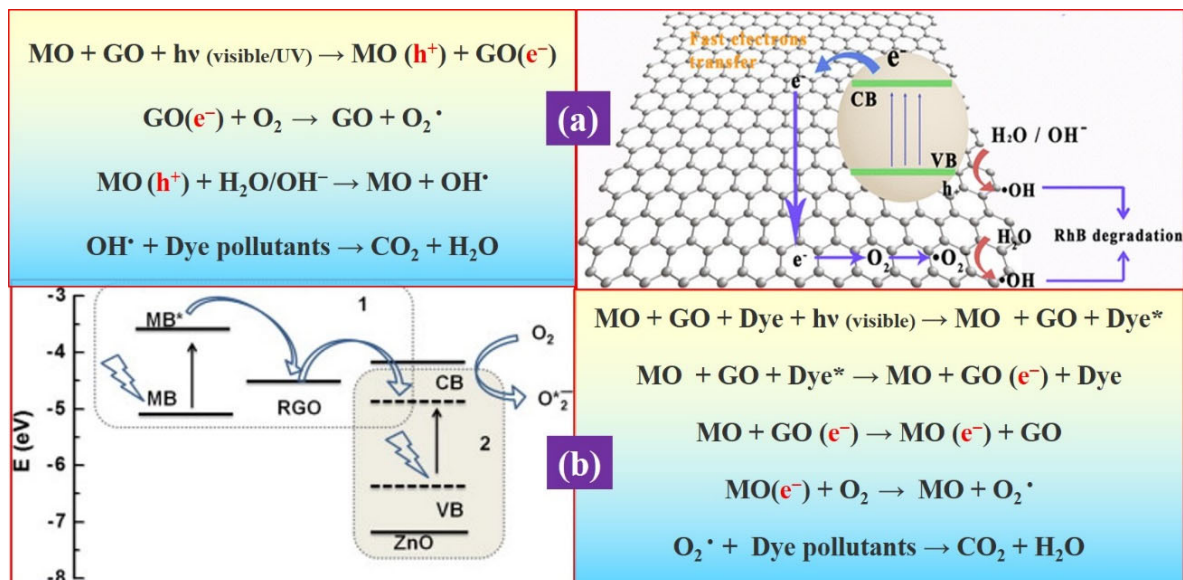


Figure 5. (a) The general chemical mechanism of photodegradation of dyes by GO–metal oxide photocatalyst showing the role of GO as a charge carrier or electron transport to enhance the photocatalytic activity of GO–metal oxide nanocomposites. Reprinted with permission from Ref. [51]) Copyright 2017-Springer. (b) The schematic of effective charge transfer by GO from dye molecules to metal oxide photocatalysts. Reprinted with permission from Ref. [52]) (MO = metal oxide semiconductor photocatalyst). Copyright 2013-Elsevier.

Photocatalyst nanomaterials composed of plasmonic [55] with GO [9,42,56,57] and/or with metal oxide photocatalysts have gained considerable attention because of the synergistic effect of surface plasmon resonance (SRP) and electron transport properties making potential candidates in various fields [53,58–61]. Recently, the role of SPR of noble metal NPs, i.e., Au or Ag, in photocatalysis has been emphasized because of their excitation under visible light, which is promising for fabricating visible light active photocatalyst materials. It enhances the activity and stability of the nanocomposite photocatalysts. SPR-induced hot-electron transfer from noble metal NPs to host materials has received considerable attention from researchers in different fields, including photocatalysis for utilizing solar energy [62–65]. Bhunia et al. [66] studied the photocatalytic activity of rGO–Ag NPs nanocomposites under both UV and visible light. It was found that Ag NPs exhibited visible-light-induced excitation of SPR-producing electron-hole pairs where the conductive rGO acted as an electron transport medium offering efficient charge separation. This leads to ROS generation, followed by the oxidative degradation of the organic pollutants, as shown in Figure 6a. Recently, Ikram et al. [67] demonstrated that Ag decorated rGO nanoflakes exhibited excellent photocatalytic activity of Ag@rGO attributed to the enhanced charge separation due to the excellent charge transport property of rGO. Similarly, Li et al. [68] studied GO–Au@Ag NPs based nanocomposites with plasmonic alloy NPs having a unique hot carrier-driven ability. The resultant photocatalytic activity of the plasmonic-based GO and nanoalloy composites were explained on the basis of the synergistic effect of alloys NPs and GO. It was proposed that alloy NPs produced high yield hot carriers on their surfaces along with enhanced localized SPR property, whereas GO provided support as a co-catalyst for photoinduced electron-transfer for promoting diverse oxidative photochemical reactions. Au/g–C₃N₄ nanosheets–rGO based for excellent visible-light photocatalysts were presented by Li et al. [69] suggesting the similar mechanism where

Au NPs exhibited the SPR effect, and rGO exhibited the electron mobility activity leading to the enhanced photocatalytic activity. Very recently, Abd-Elnaiem et al. [70] studied the various nanoarchitectures of GO and its composites with Au and ZnO. It was found that the nanocomposites exhibited higher photocatalytic activity as compared to GO due to the synergetic effect of metal and semiconductor NPs.

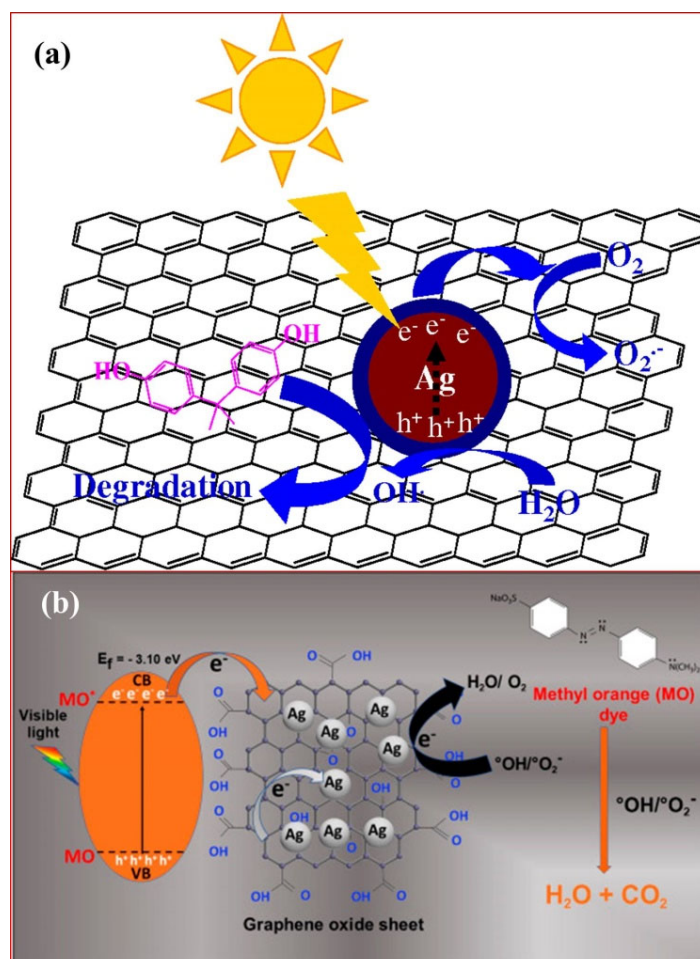


Figure 6. (a) Schematic of photocatalytic degradation mechanism by rGO–Ag NPs nanocomposites under visible light. Reprinted with permission from Ref. [66]) Copyright 2014–American Chemical Society (b) Schematic representation of the photocatalytic degradation of MO dye over Ag/rGO nanocomposite under visible-light irradiation. Reprinted with permission from Ref. [71]. Copyright 2019–Elsevier.

On the other hand, Haldarai et al. [72] and recently, Manglam et al. [71] demonstrated visible-light-driven and reusable Ag@GO nanocomposite photocatalyst as an efficient visible-light plasmonic photocatalyst. It was proposed that the dye was firstly excited to dye*, followed by an electron transfer from the dye* to GO. Then, the electron moved to Ag NPs and was trapped by O₂ to produce various ROS. The dye•+ was finally degraded by itself and/or degraded by the ROS (Figure 6b).

Recently, Manglam et al. [71] demonstrated a simple and facile method for the deposition of Ag NPs on rGO nanosheets. It can be seen in Figure 7a–c that GO nanosheets with micron size having wrinkled structures are well deposited with Ag NPs (size-80 nm) due to the strong electrostatic and electronic interaction between these nanostructures. The formation of Ag-rGO nanocomposite was also confirmed by energy dispersive X-ray spectroscopy (EDX). Its photocatalytic studies revealed the excellent photocatalytic performance of the nanocomposite in the degradation of MO with great photostability and excellent reusability that was attributed to the excellent adsorption, conductivity, and controllability.

Similarly, Haldarai et al. [72] studied the Ag@GO nanocomposite, which exhibited efficient photocatalytic activity towards photodegradation of Rhodamine 123 dye, as shown in Figure 7d–f. It was also found that after four recycles, the Ag@GO photocatalyst exhibited similar results without any considerable loss of photocatalytic activity with excellent photostability (Figure 7g). Similarly, Kumar et al. [73] studied similar Ag-GO nanocomposites for the oxidative coupling of benzyanines under visible light. These nanocomposites were highly stable and exhibited excellent photoactivity with a consistent recycling ability for several runs without any loss in activity.

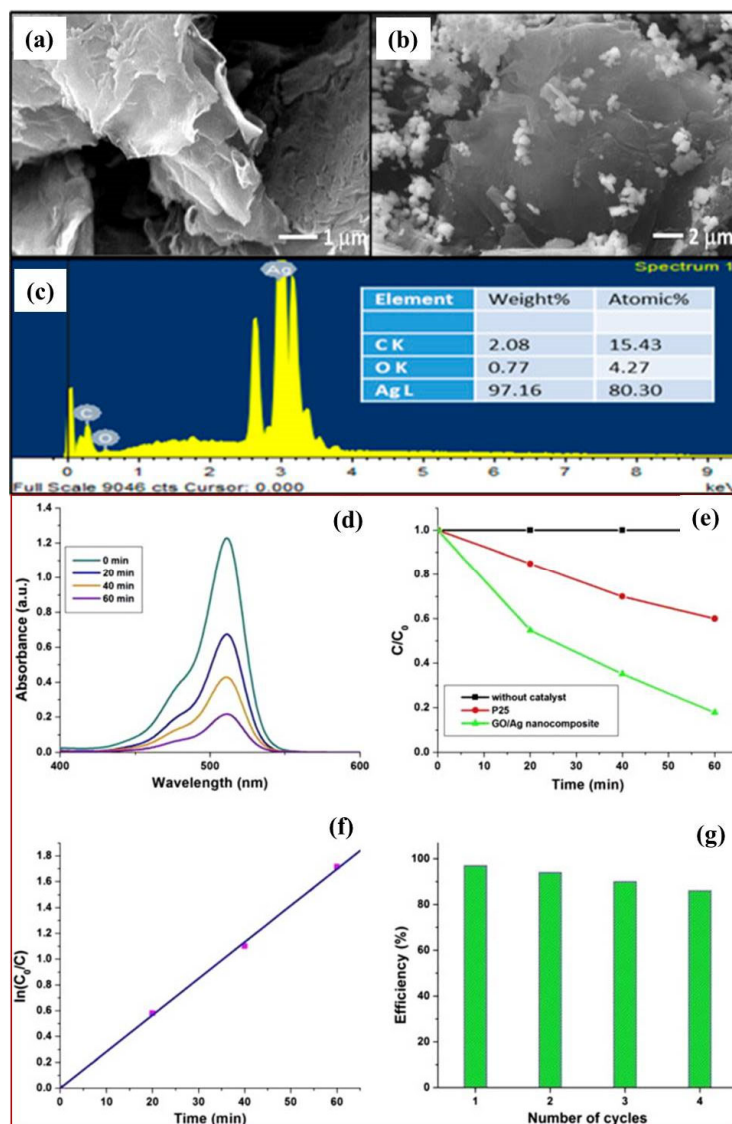


Figure 7. SEM image of (a) GO and (b) Ag/rGO nanocomposite and (c) EDX analysis of Ag/rGO nanocomposite. Reprinted with permission from Ref. [71] Copyright 2019-Elsevier. (d) UV–visible spectra of the Rhodamine 123 dye solution in the presence of photocatalyst under visible-light irradiation, (e) photodegradation of the dye, (f) first-order kinetic model for the photodegradation of dye and (g) photostability of the nanocomposite after four cycles. Reprinted with permission from Ref. [72]. Copyright 2014-Elsevier.

It has been reported that plasmonic NPs boost the efficiency of photocatalysts and act as an antenna for visible light absorption. Furthermore, GO, when coupled with plasmonic NPs and metal oxide semiconductors, exhibits greater photodegradation efficiency as compared to only metal oxide or GO–metal oxide [53,74]. In such cases, GO generally enhances

the photocatalytic activity by increasing the adsorption capacity of the nanocomposites, whereas the plasmonic NPs-metal oxide interface acts as a barrier to recombination of photoexcited charge carriers [53,74]. Al-Rawashdeh et al. [53] studied the photocatalytic activity of GO-ZnO nanocomposites with embedded Ag NPs towards photodegradation of MB dyes. It showed a better photocatalytic response after the addition of Ag NPs, which was attributed to the synergetic effect of SPR and electron mobility GO. Further, 100% photodegradation was achieved online in 40 min using this GO-ZnO nanocomposite embedded with Ag NPs. Figure 8a–d show the SEM micrographs of GO-ZnO and GO-ZnO-Ag NPs and corresponding absorbance spectra of MB dye molecules showing the better photodegradation of GO-ZnO-Ag nanocomposites. They suggested various mechanisms that could be responsible for the enhanced degradation. The large surface area of GO enhanced the adsorption of dye molecules along with the formation of π - π^* interaction between the MB dye molecules that contributed to the effective adsorption. The plasmonic NPs doping effect could minimize the recombination of photogenerated charge carriers, increasing the formation of ROS. It also led to the narrowing of the band gap of metal oxide. The mechanism is shown in Figure 8e. On the other hand, Sarkar et al. [75] studied rGO-ZnO-Ag nanocomposites and found that enhanced photocatalytic activity of this nanocomposite as compared to ZnO, Ag-ZnO or rGO-ZnO was due to an efficient charge transfer process from ZnO to both Ag and rGO as shown in Figure 8f. Very recently, Gea et al. [76] synthesized ZnO-Ag nanocomposite supported by GO with stabilized bandgap and wider visible-light region absorption for promising photocatalyst treatment of organic and textile wastewater.

Similarly, Several GO-TiO₂-Ag NPs nanocomposites systems have been studied with emphasis on the synergetic role of the GO and Ag NPs in the enhancement of photocatalytic activity [77–81]. Chen et al. [77] suggested that in photocatalytic activity of RGO-Ag-TiO₂ nanocomposites, generally visible-light-induced SPR excited electrons are injected into the CB of TiO₂, which participate in producing ROS for dye photodegradation. Furthermore, the photogenerated electrons on the CB of TiO₂ are further captured by RGO due to its extended π -conjugation structure, preventing the recombination of photogenerated charge carriers and extending their lifetime for effective generation of ROS. That is the mechanism of the overall enhanced photocatalysis activity of such nanocomposites, as shown in Figure 8g. Similarly, Qi et al. [79] exhibited that the higher performance of the Ag/GO-TiO₂ nanocomposites towards photocatalytic degradation of RhB might be attributed to its higher visible-light absorbance resulting from SPR of Ag NPs and GO. Similarly, Leong et al. [81] demonstrated the simple synthesis of rGO-Ag wrapped TiO₂ nanohybrids with controlled uniform Ag NPs. It was proposed that the wrapped rGO nanosheets triggered the electron mobility and extended the absorption of visible light absorption enhancing the photocatalytic activity in the degradation of bisphenol A due attributed to the synergetic effect of Ag NPs and rGO.

Along with the important role of GO as electron migration from the plasmonic photocatalysts containing plasmonic NPs and metal oxide photocatalyst, GO nanostructures have also been reported to play an important role in the growth of nanostructures in synthesizing excellent photocatalysts. Recently, Wang et al. [80] fabricated the GO-Ag-TiO₂ nanorods nanocomposites and studied the effect of GO interlayer on the growth of these nanostructures, surface adsorption capacity, and visible light photocatalytic activity along with SERS detection. In a recent study, Kisieleska et al. [82] studied the role of GO and rGO in in situ photocatalytically fabrication of Ag NPs embedded GO-TiO₂ and rGO-TiO₂ nanocomposite photocatalyst. It was proposed that there were two factors responsible for the growth of Ag NPs due to photogenerated electrons in TiO₂ in the presence of GO/rGO. The first factor was the number of oxygen groups on GO and rGO sheets which acted as the centers for the adsorption and nucleation of Ag ions. The other factor was the difference in the mobility of electrons within the sp³ and sp² domains in GO and rGO sheets responsible for the growth of Ag NPs.

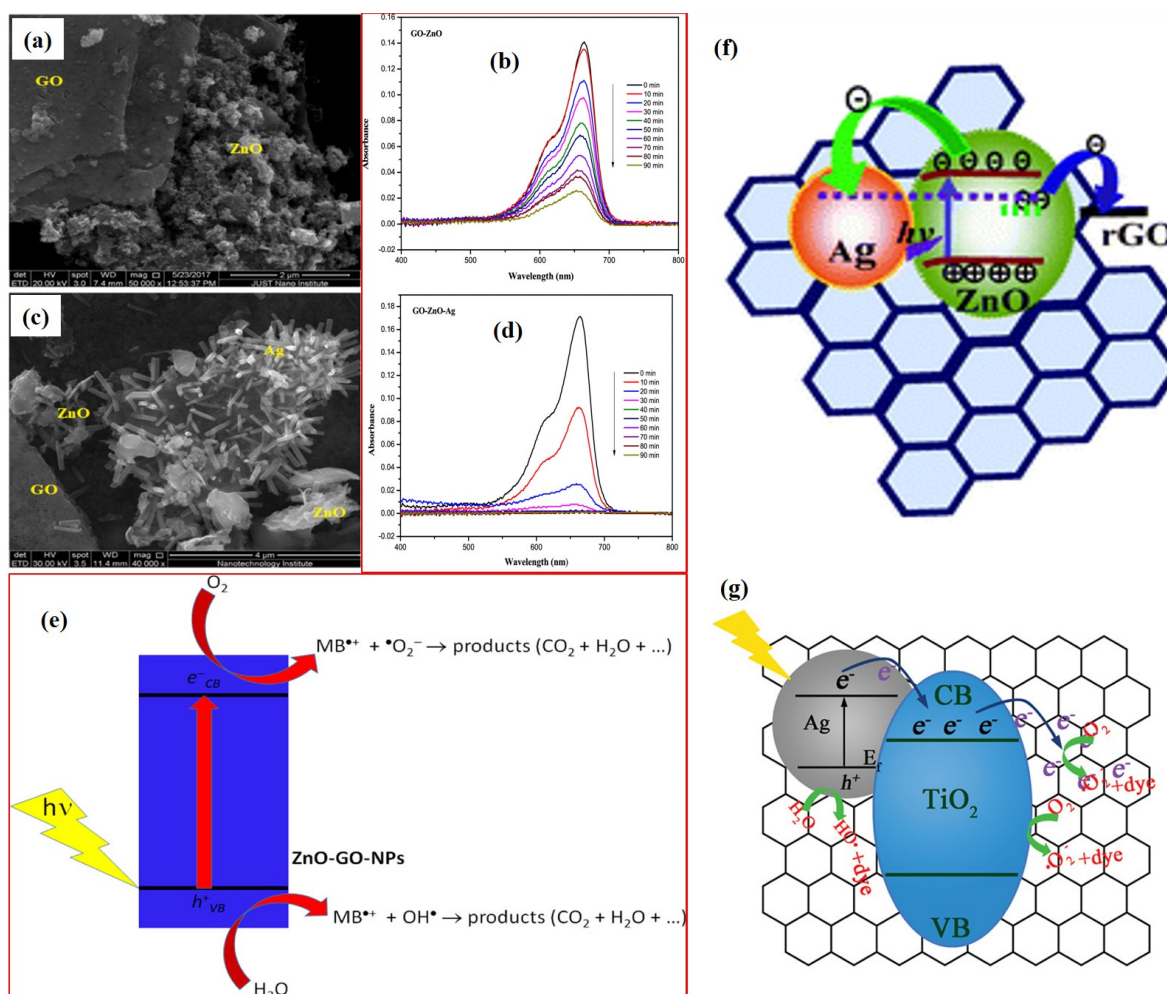


Figure 8. SEM images and corresponding photocatalytic activity of GO–ZnO (a,b), GO–ZnO–Ag (c,d) in degrading the MB dye molecules. (e) Schematic representation of mechanism of the photocatalytic degradation of MB dye molecules in case of GO–ZnO–Ag nanocomposites [53] (f) mechanism representing the charge transfer from ZnO to Ag NPs and rGO. Reprinted with permission from Ref. [75] Copyright 2013-Royal Society of Chemistry. (g) Mechanism of photocatalytic degradation of dye by RGO–Ag–TiO₂ nanocomposites. Reprinted with permission from Ref. [77]. Copyright 2018-Wiley.

3.2. As a Sole Photocatalysts

As discussed above, GO and rGO have been extensively used in photocatalysis as co-catalysts to enhance the photocatalytic activities of metal oxide photocatalysts, metals, or their nanocomposites. On the other hand, these have also been studied and researched for their sole applications as a photocatalyst and found to be a promising future sole photocatalyst material [9,23,83]. Particularly, GO and rGO have exhibited considerable results in the photodegradation of organic dye pollutants with emphasis on their utilization as standalone photocatalysts [84,85]. For example, Krishnamoorthy et al. [83] long ago investigated the photocatalytic behavior of GO by observing the change in color during the reduction of resazurin into resorufin as a function of UV irradiation time. It was observed that GO showed excellent photocatalytic activity with pseudo-first-order reaction kinetics.

In the last few years, a lot of research has been conducted to study the photocatalytic response of GO/rGO and to investigate their photocatalyst activity in the photodegradation of dye pollutants [21,23]. For example, Kumar et al. [22] chemically derived GO nanostructures through chemical oxidation of graphite for possible application in photodegradation of MB dye molecules. It showed good photocatalytic activity with a photodegradation efficiency of 60% (Figure 9a,b). It was explained that GO nanosheets exhibited a larger

surface area for the adsorption of dye molecules. It was proposed that when light interacted with a solution containing dye molecules and GO nanosheets as photocatalysts, photoexcited electrons and holes were produced due to a π - π^* excitation in the π -conjugated sp^2 domains of GO. These photogenerated electrons and holes simultaneously reacted with oxygen and water molecules to produce ROS. Eventually, ROS degraded MB dye molecules into CO_2 and H_2O molecules (Figure 9c) [22,86]. The overall reaction mechanism of GO as the sole photocatalyst is shown in Figure 9d. As can be seen in Figure 9d, when GO acts as a semiconductor, then due to the light absorption, electrons in the VB are jumped into the CB. Then photogenerated electrons and holes in CB and VB respectively produce ROS, as explained above, which further participate in photochemical degradation processes. Another mechanism could be dye induced photocatalytic mechanism similar to as explained in Figure 5b. The dye molecule can absorb the light, and excited electrons from the dye molecules can be transferred to the CB of the GO, which participates in ROS formation [22,23]. Similarly, Singh et al. [87] studied the photocatalytic activity of GO towards congo red dye along with the antibacterial activity.

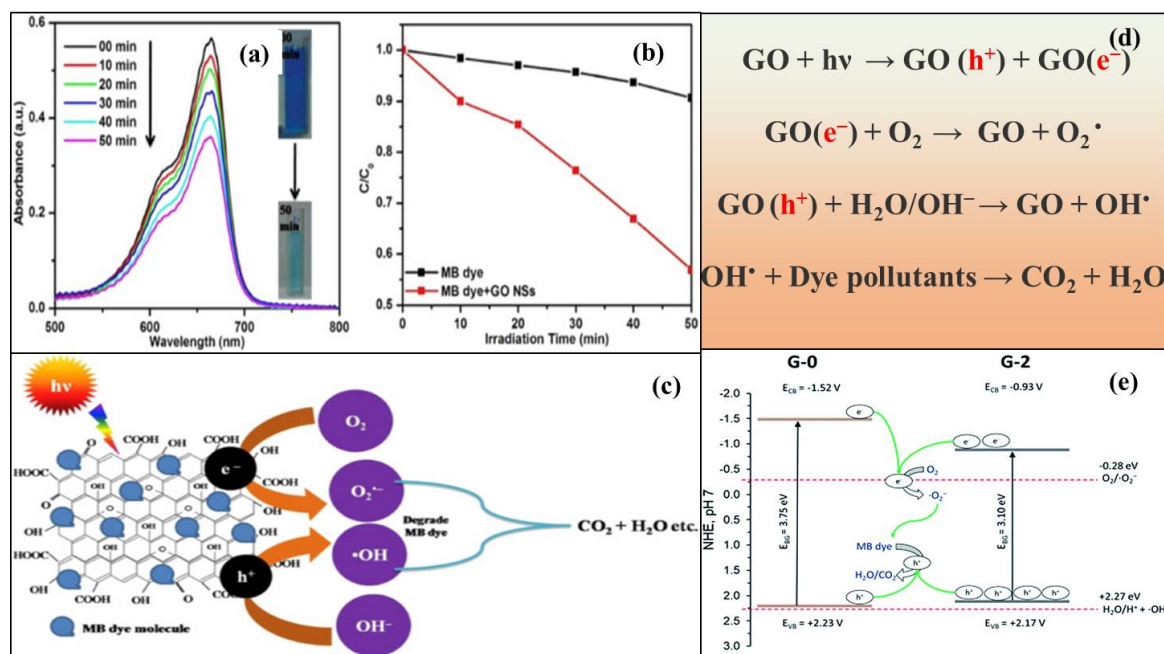


Figure 9. (a) Absorption spectra of aqueous solution of MB dye containing GO under direct sunlight at different irradiation times (b) photodegradation rate of pure MB dye solution and MB dye + GO as photocatalysts under direct sunlight irradiation. (c) Mechanism for photocatalytic degradation of MB dye with GO. Reprinted with permission from Ref. [22]. Copyright 2016-Elsevier. (d) Chemical reactions mechanism of photocatalytic action of GO in degradation of dye molecules (e) Schematic mechanism for MB photodegradation by G-0 (GO) and G-2 (rGO at optimized solvothermal process) [84].

Siong et al. [84,85] studied the photocatalytic activity of GO/rGO for the photodegradation of MB dye molecules and found that these GO nanostructures showed excellent photocatalytic performance as a metal-free photocatalyst. The higher charge carrier density, better ability to separate charge carriers, and higher photocurrent density, as well as reduced band gap, were found to be responsible for enhanced photocatalytic performance after reduction of GO to rGO. In a study, rGO was prepared at an optimized reduction temperature of 160 °C and exhibited partial restoration of the sp^2 hybridization resulting from the deoxygenation of the GO surface. It exhibited increased surface area and reduced band gap. These characteristics made it a better adsorption surface and photocatalyst, achieving more than 30% photodegradation of MB dye. It was further demonstrated that a greater adsorption removal, i.e., more than 87%, and photocatalytic degradation, i.e., more

than 98% could be achieved when 60 mg of catalyst, 50 ppm of dye at pH 11, and 60 W m^{-2} of UV-C light source were used. Similarly, in another study, rGO prepared at the optimized autoclave solvothermal reduction from GO was found to be exhibited 2.5 times greater photocatalytic activity as compared to that of GO. It was found that the band gap energy was reduced from 3.75 (GO) to 3.10 eV (rGO) due to the deoxygenation of GO resulting in defect production, as shown in Figure 9e. Similarly, Wong et al. reported the photocatalytic degradation of reactive black five dye molecules by synthesizing rGO from GO with better photoactivity [88].

However, many studies also reveal that GO does not always seem to be an efficient photocatalyst in dye degradation but shows a better effect as a co-catalyst, as experimentally shown by several reports [21,48,53,89,90]. It may be due to the wide band gap and fast recombination of photogenerated charge carriers [21]. Therefore, to overcome these issues and to make GO more efficient catalysts, doping with metal and non-metal elements has been found to be a promising technique that improves not only its charge transfer characteristics but also enhances photocatalytic performance [21,23,91]. Only a few studies have been reported modifying the photocatalytic properties of GO by doping. For example, recently, Junaid et al. [92] studied the effect of B doping in GO for enhanced optoelectronic properties and found that doped GO showed a tunable band gap from 2.91 to 3.05 eV along with enhanced electrical conductivity. It was attributed to B-induced defects, which could be promising for several applications. Singh et al. [91] demonstrated the B doping in GO and studied its photocatalytic activity for MO and MB dye photodegradation. It was found that after doping, the photocatalytic performance of GO was improved. B doped GO exhibited greater photocatalytic activity as compared to the pristine GO for MB dye molecules, as shown in Figure 10a,b. The B doped GO was found to possess semiconducting/p-type properties. These modified properties of B-doped GO were found to be more favorable for the degradation of MB (cationic dye) than MO (anionic dye). The enhanced photocatalytic performance of B doped GO was attributed to the increased density of states near Fermi level as shown in Figure 10c. Similarly, Tang et al. [93] discussed B doping in GO producing B doped rGO as visible light active nanostructures and studied its photocatalytic mechanism for the degradation of RhB dye molecules. It was found that B doped rGO exhibited better photocatalytic performance as compared to undoped GO. The RhB dye photosensitization was found to be responsible for the enhanced photoactivity of B doped rGO, where electron migration was taken place from the excited dye molecules to the B doped rGO lead to the efficient photocatalytic performance.

Recently, Tai et al. [94] demonstrated that oxygenated B groups in B doped GO could be useful for excellent photodegradation of the volatile organic compounds attributed to the high hole carrier density and p-type characteristics. In another work, the photocatalytic activity of GO was studied in the presence of an electron scavenger, which exhibited a band gap between 3.19–4.4 eV, and photocatalytic efficiency was reported three times greater than the pure GO [23]. Doping GO with transition metals could be another promising way to promote the photocatalytic activity of doped GO resulting from the enhanced charge separation and transfer induced by the interface formed between metal co-catalyst and light-harvesting GO nanostructures [21]. Khurshid et al. [21] studied the GO nanostructures doped with transition metals (Fe, Co, Ni, and Cu). It was observed that doping of metals significantly enhanced the photocurrent and also the photocatalytic activities of metal-doped GO as compared to the pristine GO. The photocatalytic mechanism of MO degradation under UV irradiation by metal doped GO photocatalysts has been shown schematically in Figure 10d. It was also concluded that Co and Ni doped Go showed excellent photocatalytic efficiencies (more than 80%) with rate constants ($k = 13 \times 10^{-3} \text{ min}^{-1}$ and $16 \times 10^{-3} \text{ min}^{-1}$), respectively, as shown in Figure 10e [21]. In this work, GO worked as a photocatalyst which showed improved activity after metal doping.

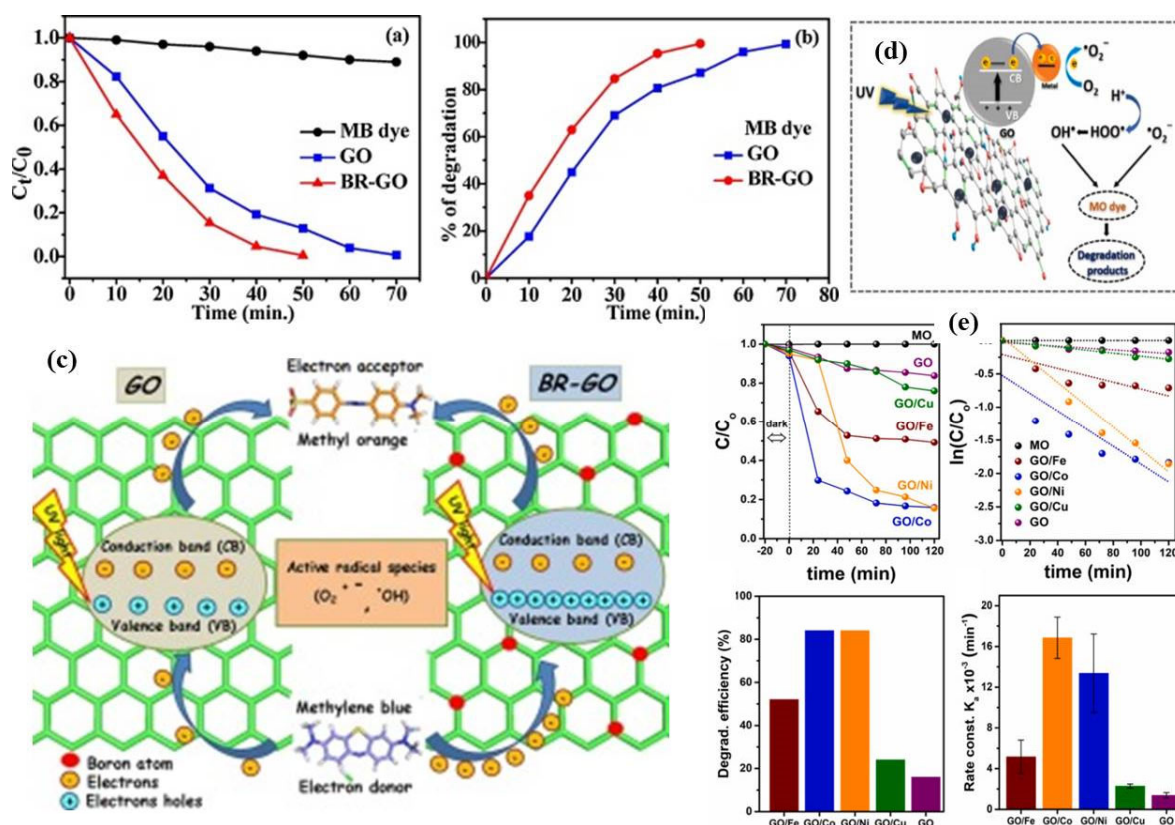


Figure 10. (a) Variation of concentration and (b) degradation efficiency with irradiation time for MB dye. (c) Schematic representation of the complete degradation process. Reprinted with permission from Ref. [91]. Copyright 2018-Elsevier. (d) Photocatalytic mechanism of MO degradation under UV irradiation by metal doped GO photocatalysts (e) MO degradation vs. time curves showing first-order pseudo kinetics, degradation efficiencies, and rate constants of GO/Fe, GO/Co, GO/Ni, GO/Cu, and pristine GO. Reprinted with permission from Ref. [21] Copyright 2021-Elsevier.

The above discussion reveals that GO is not only a potential candidate to act as a co-catalyst but also has great potential to be an efficient sole photocatalyst. A comparative of photocatalytic activity of GO-based photocatalysts and different roles of GO along with important achievements/mechanisms in photodegradation of organic dye pollutants have been summarized in Table 1 from the latest research results in the literature. All these are attributed to the excellent surface and optoelectronic properties of GO contributing to a better charge transfer mechanism, which makes it a more attractive photocatalyst, as shown in the schematic of Figure 11.

Table 1. A comparative of photocatalytic activity of GO based photocatalysts and different roles of GO along with important achievements/mechanisms in photodegradation of organic dye pollutants.

S. No	GO Based Photocatalysts	Role of GO	Uv/Visible Radiation/Other Conditions	Organic Dye Pollutants	Results/Photocatalytic Efficiency/Rate	Ref.
1.	Co and Ni-modified GO	Sole photocatalyst	UV light	MO	Metal doping improved the properties resulting in high photocurrent, photodegradation efficiency ~84%. Rate constants = $13 \times 10^{-3} \text{ min}^{-1}$ and $16 \times 10^{-3} \text{ min}^{-1}$.	[21]
2.	GO nanosheets	Sole photocatalyst	Visible light	MB	Photodegradation efficiency 60%.	[22]

Table 1. Cont.

S. No	GO Based Photocatalysts	Role of GO	Uv/Visible Radiation/Other Conditions	Organic Dye Pollutants	Results/Photocatalytic Efficiency/Rate	Ref.
3.	Single layer GO modified by electron scavenger	Sole photocatalyst	UV light	MO	Band gap = 3.19–4.4 eV, photocatalytic efficiency was 24% and enhanced 3 times greater in presence of electron scavenger	[23]
4.	ZnO-GO nanocomposites	Co-catalyst	Under the darkness ultrasound-driven piezoelectric catalysis effect, visible light	MB, RhB and MO	ZnO-GO nanocomposites exhibit stronger piezoelectric catalytic activity compared with the pure ZnO, formation of ROS	[43]
5.	GO-ZnO nanorods	Co-catalyst	UV light	MB	Excellent photoactivity due to strong interface coupling between ZnO and Go	[45]
6.	GO-TiO ₂ nanocomposite	Co-catalyst	Near-UV/Vis and visible light.	DP	Higher photocatalytic degradation efficiency as compared to bare TiO ₂ and rate of $83.9 \times 10^{-3} \text{ min}^{-1}$	[46]
7.	GO-ZnO nanocomposite	Co-catalyst	UV light	MB	Photodegradation efficiency ~80% in 70 min, interface interactions, photo-induced charge transfer interactions, high performance and recyclability	[47]
8.	ZnO-GO nanocomposite	Co-catalyst	UV light	MB	Photodegradation efficiency 97.6% in 90 min and the first-order reaction rate 0.04401 min^{-1} .	[48]
9.	GO-TiO ₂ nanocomposite	Adsorbent, electron acceptor and photosensitizer	UV and visible light	MB	Photodegradation efficiency of 90 and 95% with rate of 72.25×10^{-3} and $23.66 \times 10^{-3} \text{ min}^{-1}$ for under UV and visible light respectively	[49]
10.	TiO ₂ -rGO nanocomposites	Co-catalyst	Visible light	RhB, phenol	Photodegradation efficiency 85% for RhB in 90 min, 100% degradation of phenol in 150 min, strong interfacial contact and charge separation.	[51]
11.	GO-ZnO-Cu/Ag nanocomposite	Co-catalyst	Sunlight	MB	Catalytic activity of 84% (Cu) 100% after 40 min (Ag) rate constant of 0.1112 min^{-1}	[53]
12.	GO and Ag@rGO nanocomposite	Both	Visible light	MB	% degradation up to 100% in 120 min. rate 0.1300 min^{-1} (GO) to 0.7459 min^{-1} (Ag@rGO)	[67]
13.	Au@Ag/GO nanocomposite	Co-catalyst	Visible light	tetracycline hydrochloride	99.36% photodegradation in 70 min.	[68]
14.	Au/g-C ₃ N ₄ /rGO	Co-catalyst	Visible light	MB	Photodegradation rate 6 times higher than pure g-C ₃ N ₄	[69]
15.	porous GO, Au-RGO, and GO-Au-ZnO nanocomposite	Porous GO as sole catalysts	UV-visible light	MB	Highest Photodegradation efficiency 97% for porous GO with rate constant $20.0 \times 10^{-3} \text{ min}^{-1}$	[70]
16.	GO and Ag/rGO	Co-catalyst	Visible light	MO	Photodegradation rate for Ag/rGO was 0.048 min^{-1} and, for GO it was 0.02 min^{-1}	[71]
17.	ZnO-Ag-GO	Co-catalyst	Visible light	-	Band gap of 2.75 eV	[76]
18.	Ag-modified GO-TiO ₂	Co-catalyst	Sunlight	RhB	100% RhB removal in 180 min with rate constant of $4.65 \times 10^{-3} \text{ min}^{-1}$	[79]

Table 1. Cont.

S. No	GO Based Photocatalysts	Role of GO	Uv/Visible Radiation/Other Conditions	Organic Dye Pollutants	Results/Photocatalytic Efficiency/Rate	Ref.
19.	rGO nanosheet	Sole catalyst	UV-light	MB	Band gap = 3.10 eV, the pseudo-first order rate constant of rGO was 0.070 h^{-1} which was remarkably 2.5 times higher than the pristine GO with rate 0.028 h^{-1} .	[84]
20.	rGO nanosheet	Sole catalyst	UV-light	MB	Photocatalytic degradation efficiency of 98.57% with rate 0.711 h^{-1}	[85]
21.	GO nanosheet	Sole catalyst	UV-light	Congo red (CR)	Photodegradatin efficiency more than 90% in 120 min with rate constant of 0.0359 min^{-1}	[87]
22.	B doped GO	Sole catalyst	UV-light	MB and MO	Band gap of GO and B doped GO was 2.8 eV and 3.00 eV respectively. MB dye degradation 100% in 50 min by doped GO while 70% by GO. MO degradation 100% in 100 min by doped GO while 50% only by GO.	[91]
23.	B doped GO	Sole catalyst	UV-light	VoCs	Remove 80% of the VoCs within 6 h (0.283 h^{-1})	[94]
24.	B doped rGO	Sole catalyst	Visible light	RhB	B doped rGO showed significantly higher photocatalytic activity than non-doped RGO	[93]

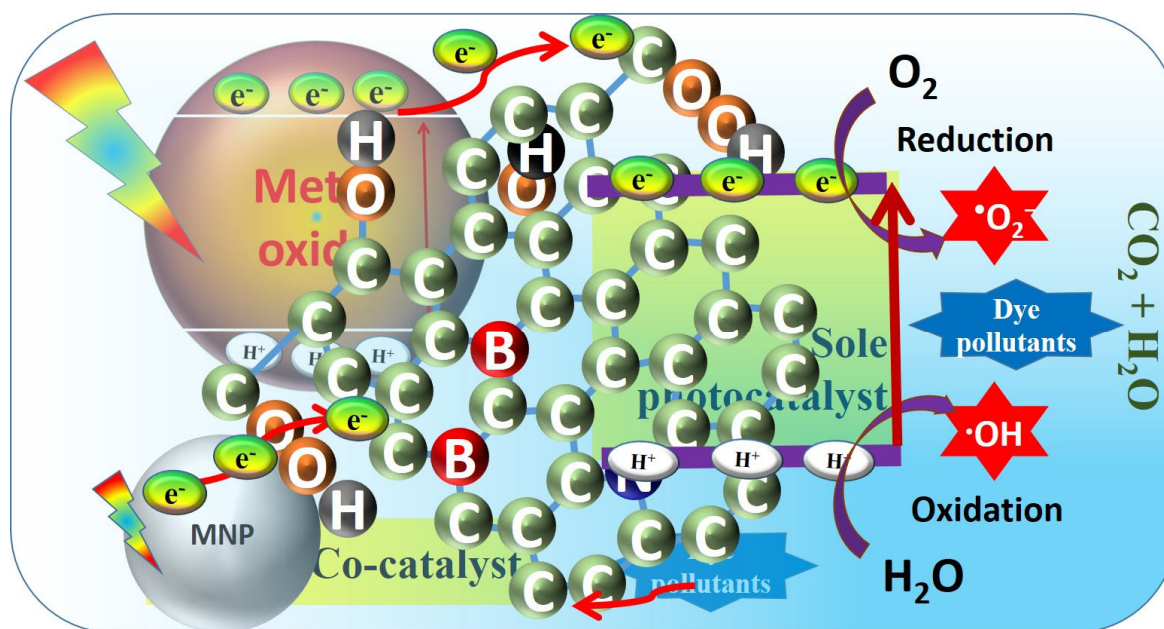


Figure 11. Schematic of various charge transfer mechanism of GO in photocatalytic degradation of dye pollutants including role of GO as a co-catalyst with metal oxide photocatalysts for charge separation and as a sole photocatalyst with semiconductor characteristics.

4. Summary and Future Prospects

Photocatalyst nanomaterials are promising for various processes in the environment utilizing sunlight, and photocatalytic degradation of organic dye pollutants is one of the important aspects of wastewater treatment. In the last few years, a lot of progress in this field has been made, including synthesis techniques, the development of new photocatalysts nanomaterials, and the mechanism of their photocatalytic action. GO is one of such nanomaterials which has been studied in many aspects of photocatalytic degradation of dye pollutants. Here, particularly, mechanistic insights into GO-driven photocatalysis as co-catalyst (with most used photocatalysts, i.e., TiO₂ and ZnO, or with plasmonic nanocomposites) have been discussed in the degradation of organic dye pollutants. Furthermore, it has emerged as a potential sole photocatalyst nanomaterial with semiconductor features. It has shown fascinating photocatalytic properties and a simple mechanism for photocatalytic degradation of organic dye pollutants, which have been discussed in the present review article.

Recent developments in research related to the photocatalytic activity of GO show its potential to be an efficient photocatalyst material. It has been emerging as a carbon-based photocatalyst with a metal-free characteristic that could be explored to serve as a sole photocatalyst. Based on the current status of GO in the field of photocatalysis, it can be assumed that continuous research on these materials will lead to providing more tunability in its semiconducting properties. This is still a great challenge, along with the stability for GO, which needs to be explored in future research. It has been used potentially as a co-catalyst only to enhance the performance of the other semiconductors. Even as a co-catalyst, it has not been explored as a co-photocatalyst that does not exhibit its potential. It has tunable characteristics, especially the band gap, which makes it a more efficient photocatalyst. In combination with other metal oxide photocatalysts, it could add to the photocatalytic activity by the synergetic effect of photocatalytic action as well as co-catalyst by producing and transporting photoexcited electrons, respectively. This is another scope for GO nanostructures to be explored in future research. In this context, chemical doping is one of the simple techniques to boost the photocatalytic efficiency of the GO. It also needs to be explored from a photocatalytic point of view to enhance the photocatalytic activity of GO as a sole photocatalyst as well as in the role of a co-catalyst. The band gap engineering of GO will definitely enhance its optoelectronic properties, which will enhance its potential application as not only a sole photocatalyst but also its co-photocatalyst activity. It will strengthen the understanding of the role of GO in photocatalytic action from a more fundamental point of view, which could be explored in a more excellent way. The author thinks that this review will provide a more basic understanding of the photocatalytic action of GO. It is also expected that the scientific community will explore the mode of action of GO and GO-based photocatalyst nanocomposites to the next level of understanding.

Funding: This research received no external funding.

Institutional Review Board Statement: Not applicable.

Informed Consent Statement: Not applicable.

Data Availability Statement: Not applicable.

Acknowledgments: Author would like to thank Samriti and Jagdish for performing related experimental work. Author also acknowledges Department of Science and Technology (DST) India for INSPIRE Faculty award.

Conflicts of Interest: The authors declare no conflict of interest.

References

1. Sharma, P.; Prakash, J.; Kaushal, R. An insight into the green synthesis of SiO₂ nanostructures as a novel adsorbent for removal of toxic water pollutants. *Environ. Res.* **2022**, *212*, 113328. [[CrossRef](#)] [[PubMed](#)]
2. Balasubramaniam, B.; Singh, N.; Kar, P.; Tyagi, A.; Prakash, J.; Gupta, R.K. Engineering of transition metal dichalcogenide-based 2D nanomaterials through doping for environmental applications. *Mol. Syst. Des. Eng.* **2019**, *4*, 804–827. [[CrossRef](#)]

3. Prakash, J.; Harris, R.A.; Swart, H.C. Embedded plasmonic nanostructures: Synthesis, fundamental aspects and their surface enhanced Raman scattering applications. *Int. Rev. Phys. Chem.* **2016**, *35*, 353–398. [[CrossRef](#)]
4. Chakraborty, A.; Samriti; Ruzimuradov, O.; Gupta, R.K.; Cho, J.; Prakash, J. TiO₂ nanoflower photocatalysts: Synthesis, modifications and applications in wastewater treatment for removal of emerging organic pollutants. *Environ. Res.* **2022**, *212*, 113550. [[CrossRef](#)]
5. Sharma, P.; Prakash, J.; Palai, T.; Kaushal, R. Surface functionalization of bamboo leave mediated synthesized SiO₂ nanoparticles: Study of adsorption mechanism, isotherms and enhanced adsorption capacity for removal of Cr (VI) from aqueous solution. *Environ. Res.* **2022**, *214*, 113761. [[CrossRef](#)]
6. Prakash, J.; Sun, S.; Swart, H.C.; Gupta, R.K. Noble metals-TiO₂ nanocomposites: From fundamental mechanisms to photocatalysis, surface enhanced Raman scattering and antibacterial applications. *Appl. Mater. Today* **2018**, *11*, 82–135. [[CrossRef](#)]
7. Chen, Z.; Zhang, G.; Chen, H.; Prakash, J.; Zheng, Y.; Sun, S. Multi-metallic catalysts for the electroreduction of carbon dioxide: Recent advances and perspectives. *Renew. Sustain. Energy Rev.* **2022**, *155*, 111922. [[CrossRef](#)]
8. Prakash, J.; Kumar, P.; Harris, R.A.; Swart, C.; Neethling, J.H.; van Vuuren, A.J.; Swart, H.C. Synthesis, characterization and multifunctional properties of plasmonic Ag–TiO₂ nanocomposites. *Nanotechnology* **2016**, *27*, 355707. [[CrossRef](#)]
9. Samriti; Manisha; Chen, Z.; Sun, S.; Prakash, J. Design and engineering of graphene nanostructures as independent solar-driven photocatalysts for emerging applications in the field of energy and environment. *Mol. Syst. Des. Eng.* **2022**, *7*, 213–238. [[CrossRef](#)]
10. Singh, N.; Prakash, J.; Gupta, R.K. Design and engineering of high-performance photocatalytic systems based on metal oxide–graphene–noble metal nanocomposites. *Mol. Syst. Des. Eng.* **2017**, *2*, 422–439. [[CrossRef](#)]
11. Prakash, J.; Samriti; Kumar, A.; Dai, H.; Janegitz, B.C.; Krishnan, V.; Swart, H.C.; Sun, S. Novel rare earth metal–doped one-dimensional TiO₂ nanostructures: Fundamentals and multifunctional applications. *Mater. Today Sustain.* **2021**, *13*, 100066. [[CrossRef](#)]
12. Singh, N.; Prakash, J.; Misra, M.; Sharma, A.; Gupta, R.K. Dual Functional Ta-Doped Electrospun TiO₂ Nanofibers with Enhanced Photocatalysis and SERS Detection for Organic Compounds. *ACS Appl. Mater. Interfaces* **2017**, *9*, 28495–28507. [[CrossRef](#)] [[PubMed](#)]
13. Prakash, J.; Pivin, J.C.; Swart, H.C. Noble metal nanoparticles embedding into polymeric materials: From fundamentals to applications. *Adv. Colloid Interface Sci.* **2015**, *226*, 187–202. [[CrossRef](#)] [[PubMed](#)]
14. Lu, K.-Q.; Li, Y.-H.; Tang, Z.-R.; Xu, Y.-J. Roles of Graphene Oxide in Heterogeneous Photocatalysis. *ACS Mater. Au* **2021**, *1*, 37–54. [[CrossRef](#)]
15. Samriti; Rajput, V.; Gupta, R.K.; Prakash, J. Engineering metal oxide semiconductor nanostructures for enhanced charge transfer: Fundamentals and emerging SERS applications. *J. Mater. Chem. C* **2022**, *10*, 73–95. [[CrossRef](#)]
16. Prakash, J. Fundamentals and applications of recyclable SERS substrates. *Int. Rev. Phys. Chem.* **2019**, *38*, 201–242. [[CrossRef](#)]
17. Jamjoum, H.A.A.; Umar, K.; Adnan, R.; Razali, M.R.; Mohamad Ibrahim, M.N. Synthesis, Characterization, and Photocatalytic Activities of Graphene Oxide/metal Oxides Nanocomposites: A Review. *Front. Chem.* **2021**, *9*, 752276. [[CrossRef](#)]
18. Raizada, P.; Sudhaik, A.; Singh, P. Photocatalytic water decontamination using graphene and ZnO coupled photocatalysts: A review. *Mater. Sci. Energy Technol.* **2019**, *2*, 509–525. [[CrossRef](#)]
19. Lin, Y.-P.; Ksari, Y.; Prakash, J.; Giovanelli, L.; Valmalette, J.-C.; Themlin, J.-M. Nitrogen-doping processes of graphene by a versatile plasma-based method. *Carbon* **2014**, *73*, 216–224. [[CrossRef](#)]
20. Yang, X.; Zhang, G.; Prakash, J.; Chen, Z.; Gauthier, M.; Sun, S. Chemical vapour deposition of graphene: Layer control, the transfer process, characterisation, and related applications. *Int. Rev. Phys. Chem.* **2019**, *38*, 149–199. [[CrossRef](#)]
21. Khurshid, F.; Jeyavelan, M.; Nagarajan, S. Photocatalytic dye degradation by graphene oxide doped transition metal catalysts. *Synth. Met.* **2021**, *278*, 116832. [[CrossRef](#)]
22. Kumar, S.; Kumar, A. Chemically derived luminescent graphene oxide nanosheets and its sunlight driven photocatalytic activity against methylene blue dye. *Opt. Mater.* **2016**, *62*, 320–327. [[CrossRef](#)]
23. Govindan, K.; Suresh, A.K.; Sakthivel, T.; Murugesan, K.; Mohan, R.; Gunasekaran, V.; Jang, A. Effect of peroxomonosulfate, peroxodisulfate and hydrogen peroxide on graphene oxide photocatalytic performances in methyl orange dye degradation. *Chemosphere* **2019**, *237*, 124479. [[CrossRef](#)]
24. Putri, L.K.; Ong, W.-J.; Chang, W.S.; Chai, S.-P. Heteroatom doped graphene in photocatalysis: A review. *Appl. Surf. Sci.* **2015**, *358*, 2–14. [[CrossRef](#)]
25. Shen, Y.; Yang, S.; Zhou, P.; Sun, Q.; Wang, P.; Wan, L.; Li, J.; Chen, L.; Wang, X.; Ding, S.; et al. Evolution of the band-gap and optical properties of graphene oxide with controllable reduction level. *Carbon* **2013**, *62*, 157–164. [[CrossRef](#)]
26. Abid; Sehwat, P.; Islam, S.S.; Mishra, P.; Ahmad, S. Reduced graphene oxide (rGO) based wideband optical sensor and the role of Temperature, Defect States and Quantum Efficiency. *Sci. Rep.* **2018**, *8*, 3537. [[CrossRef](#)] [[PubMed](#)]
27. Komba, N.; Zhang, G.; Wei, Q.; Yang, X.; Prakash, J.; Chenitz, R.; Rosei, F.; Sun, S. Iron (II) phthalocyanine/N-doped graphene: A highly efficient non-precious metal catalyst for oxygen reduction. *Int. J. Hydrogen Energy* **2019**, *44*, 18103–18114. [[CrossRef](#)]
28. Farjadian, F.; Abbaspour, S.; Sadatlu, M.A.A.; Mirkiani, S.; Ghasemi, A.; Hoseini-Ghahfarokhi, M.; Mozaffari, N.; Karimi, M.; Hamblin, M.R. Recent Developments in Graphene and Graphene Oxide: Properties, Synthesis, and Modifications: A Review. *ChemistrySelect* **2020**, *5*, 10200–10219. [[CrossRef](#)]
29. Ali, I.; Basheer, A.A.; Mbianda, X.Y.; Burakov, A.; Galunin, E.; Burakova, I.; Mkrtychyan, E.; Tkachev, A.; Grachev, V. Graphene based adsorbents for remediation of noxious pollutants from wastewater. *Environ. Int.* **2019**, *127*, 160–180. [[CrossRef](#)]

30. Mei, X.; Meng, X.; Wu, F. Hydrothermal method for the production of reduced graphene oxide. *Phys. E Low-Dimens. Syst. Nanostructures* **2015**, *68*, 81–86. [[CrossRef](#)]
31. Putri, L.K.; Ng, B.-J.; Ong, W.-J.; Lee, H.W.; Chang, W.S.; Chai, S.-P. Heteroatom Nitrogen- and Boron-Doping as a Facile Strategy to Improve Photocatalytic Activity of Standalone Reduced Graphene Oxide in Hydrogen Evolution. *ACS Appl. Mater. Interfaces* **2017**, *9*, 4558–4569. [[CrossRef](#)] [[PubMed](#)]
32. Prakash, J.; Tripathi, A.; Khan, S.A.; Pivin, J.C.; Singh, F.; Tripathi, J.; Kumar, S.; Avasthi, D.K. Ion beam induced interface mixing of Ni on PTFE bilayer system studied by quadrupole mass analysis and electron spectroscopy for chemical analysis. *Vacuum* **2010**, *84*, 1275–1279. [[CrossRef](#)]
33. Prakash, J.; Swart, H.C.; Zhang, G.; Sun, S. Emerging applications of atomic layer deposition for the rational design of novel nanostructures for surface-enhanced Raman scattering. *J. Mater. Chem. C* **2019**, *7*, 1447–1471. [[CrossRef](#)]
34. Prakash, J.; Kumar, V.; Erasmus, L.J.B.; Duvenhage, M.M.; Sathiyar, G.; Bellucci, S.; Sun, S.; Swart, H.C. Phosphor Polymer Nanocomposite: ZnO:Tb³⁺ Embedded Polystyrene Nanocomposite Thin Films for Solid-State Lighting Applications. *ACS Appl. Nano Mater.* **2018**, *1*, 977–988. [[CrossRef](#)]
35. Singh, J.P.; Chen, C.L.; Dong, C.L.; Prakash, J.; Kabiraj, D.; Kanjilal, D.; Pong, W.F.; Asokan, K. Role of surface and subsurface defects in MgO thin film: XANES and magnetic investigations. *Superlattices Microstruct.* **2015**, *77*, 313–324. [[CrossRef](#)]
36. Chen, Z.; Zhang, G.; Prakash, J.; Zheng, Y.; Sun, S. Rational Design of Novel Catalysts with Atomic Layer Deposition for the Reduction of Carbon Dioxide. *Adv. Energy Mater.* **2019**, *9*, 1900889. [[CrossRef](#)]
37. Kumar, P.; Chandra Mathpal, M.; Prakash, J.; Viljoen, B.C.; Roos, W.D.; Swart, H.C. Band gap tailoring of cauliflower-shaped CuO nanostructures by Zn doping for antibacterial applications. *J. Alloy. Compd.* **2020**, *832*, 154968. [[CrossRef](#)]
38. Pathak, T.K.; Kumar, V.; Prakash, J.; Purohit, L.P.; Swart, H.C.; Kroon, R.E. Fabrication and characterization of nitrogen doped p-ZnO on n-Si heterojunctions. *Sens. Actuators A Phys.* **2016**, *247*, 475–481. [[CrossRef](#)]
39. Prakash, J.; Singh, A.; Sathiyar, G.; Ranjan, R.; Singh, A.; Garg, A.; Gupta, R.K. Progress in tailoring perovskite based solar cells through compositional engineering: Materials properties, photovoltaic performance and critical issues. *Mater. Today Energy* **2018**, *9*, 440–486. [[CrossRef](#)]
40. Gupta, T.; Samriti; Cho, J.; Prakash, J. Hydrothermal synthesis of TiO₂ nanorods: Formation chemistry, growth mechanism, and tailoring of surface properties for photocatalytic activities. *Mater. Today Chem.* **2021**, *20*, 100428. [[CrossRef](#)]
41. Kumar, V.; Prakash, J.; Singh, J.P.; Chae, K.H.; Swart, C.; Ntwaeaborwa, O.M.; Swart, H.C.; Dutta, V. Role of silver doping on the defects related photoluminescence and antibacterial behaviour of zinc oxide nanoparticles. *Colloids Surf. B Biointerfaces* **2017**, *159*, 191–199. [[CrossRef](#)] [[PubMed](#)]
42. Mathivanan, D.; Shalini Devi, K.S.; Sathiyar, G.; Tyagi, A.; da Silva, V.A.O.P.; Janegitz, B.C.; Prakash, J.; Gupta, R.K. Novel polypyrrole-graphene oxide-gold nanocomposite for high performance hydrogen peroxide sensing application. *Sens. Actuators A Phys.* **2021**, *328*, 112769. [[CrossRef](#)]
43. Ma, W.; Lv, M.; Cao, F.; Fang, Z.; Feng, Y.; Zhang, G.; Yang, Y.; Liu, H. Synthesis and characterization of ZnO-GO composites with their piezoelectric catalytic and antibacterial properties. *J. Environ. Chem. Eng.* **2022**, *10*, 107840. [[CrossRef](#)]
44. Yeh, T.-F.; Cihlář, J.; Chang, C.-Y.; Cheng, C.; Teng, H. Roles of graphene oxide in photocatalytic water splitting. *Mater. Today* **2013**, *16*, 78–84. [[CrossRef](#)]
45. Shaheen, S.; Iqbal, A.; Ikram, M.; Imran, M.; Naz, S.; Ul-Hamid, A.; Shahzadi, A.; Nabgan, W.; Haider, J.; Haider, A. Graphene oxide-ZnO nanorods for efficient dye degradation, antibacterial and in-silico analysis. *Appl. Nanosci.* **2022**, *12*, 165–177. [[CrossRef](#)]
46. Pastrana-Martínez, L.M.; Morales-Torres, S.; Likodimos, V.; Falaras, P.; Figueiredo, J.L.; Faria, J.L.; Silva, A.M.T. Role of oxygen functionalities on the synthesis of photocatalytically active graphene-TiO₂ composites. *Appl. Catal. B Environ.* **2014**, *158–159*, 329–340. [[CrossRef](#)]
47. Víctor-Román, S.; García-Bordejé, E.; Hernández-Ferrer, J.; González-Domínguez, J.M.; Ansón-Casaos, A.; Silva, A.M.T.; Maser, W.K.; Benito, A.M. Controlling the surface chemistry of graphene oxide: Key towards efficient ZnO-GO photocatalysts. *Catal. Today* **2020**, *357*, 350–360. [[CrossRef](#)]
48. Lin, Y.; Hong, R.; Chen, H.; Zhang, D.; Xu, J. Green Synthesis of ZnO-GO Composites for the Photocatalytic Degradation of Methylene Blue. *J. Nanomater.* **2020**, *2020*, 4147357. [[CrossRef](#)]
49. Nguyen-Phan, T.-D.; Pham, V.H.; Shin, E.W.; Pham, H.-D.; Kim, S.; Chung, J.S.; Kim, E.J.; Hur, S.H. The role of graphene oxide content on the adsorption-enhanced photocatalysis of titanium dioxide/graphene oxide composites. *Chem. Eng. J.* **2011**, *170*, 226–232. [[CrossRef](#)]
50. Micochova, P.; Chadha, A.; Hesselöj, T.; Fraternali, F.; Ramsden, J.; Gupta, R. Rapid inactivation of SARS-CoV-2 by titanium dioxide surface coating [version 2; peer review: 2 approved]. *Wellcome Open Res.* **2021**, *6*, 56. [[CrossRef](#)]
51. Iqbal, W.; Tian, B.; Anpo, M.; Zhang, J. Single-step solvothermal synthesis of mesoporous anatase TiO₂-reduced graphene oxide nanocomposites for the abatement of organic pollutants. *Res. Chem. Intermed.* **2017**, *43*, 5187–5201. [[CrossRef](#)]
52. Tien, H.N.; Luan, V.H.; Hoa, L.T.; Khoa, N.T.; Hahn, S.H.; Chung, J.S.; Shin, E.W.; Hur, S.H. One-pot synthesis of a reduced graphene oxide-zinc oxide sphere composite and its use as a visible light photocatalyst. *Chem. Eng. J.* **2013**, *229*, 126–133. [[CrossRef](#)]
53. Al-Rawashdeh, N.A.F.; Allabadi, O.; Aljarrah, M.T. Photocatalytic Activity of Graphene Oxide/Zinc Oxide Nanocomposites with Embedded Metal Nanoparticles for the Degradation of Organic Dyes. *ACS Omega* **2020**, *5*, 28046–28055. [[CrossRef](#)] [[PubMed](#)]

54. Oppong, S.O.-B.; Anku, W.W.; Shukla, S.K.; Agorku, E.S.; Govender, P.P. Photocatalytic degradation of indigo carmine using Nd-doped TiO₂-decorated graphene oxide nanocomposites. *J. Sol-Gel Sci. Technol.* **2016**, *80*, 38–49. [[CrossRef](#)]
55. Kumar, P.; Chandra Mathpal, M.; Jagannath, G.; Prakash, J.; Maze, J.-R.; Roos, W.D.; Swart, H.C. Optical limiting applications of resonating plasmonic Au nanoparticles in a dielectric glass medium. *Nanotechnology* **2021**, *32*, 345709. [[CrossRef](#)]
56. Tong, X.; Zhang, G.; Prakash, J.; Sun, S. 3D Graphene and Its Nanocomposites: From Synthesis to Multifunctional Applications. In *Graphene Functionalization Strategies: From Synthesis to Applications*; Khan, A., Jawaaid, M., Neppolian, B., Asiri, A.M., Eds.; Springer: Singapore, 2019; pp. 363–388.
57. Verma, S.; Mal, D.S.; de Oliveira, P.R.; Janegitz, B.C.; Prakash, J.; Gupta, R.K. A facile synthesis of novel polyaniline/graphene nanocomposite thin films for enzyme-free electrochemical sensing of hydrogen peroxide. *Mol. Syst. Des. Eng.* **2022**, *7*, 158–170. [[CrossRef](#)]
58. Prakash, J.; Kumar, V.; Kroon, R.E.; Asokan, K.; Rigato, V.; Chae, K.H.; Gautam, S.; Swart, H.C. Optical and surface enhanced Raman scattering properties of Au nanoparticles embedded in and located on a carbonaceous matrix. *Phys. Chem. Chem. Phys.* **2016**, *18*, 2468–2480. [[CrossRef](#)]
59. Kumar, P.; Chandra Mathpal, M.; Prakash, J.; Jagannath, G.; Roos, W.D.; Swart, H.C. Plasmonic and nonlinear optical behavior of nanostructures in glass matrix for photonics application. *Mater. Res. Bull.* **2020**, *125*, 110799. [[CrossRef](#)]
60. Prakash, J.; Tripathi, A.; Gautam, S.; Chae, K.H.; Song, J.; Rigato, V.; Tripathi, J.; Asokan, K. Phenomenological understanding of dewetting and embedding of noble metal nanoparticles in thin films induced by ion irradiation. *Mater. Chem. Phys.* **2014**, *147*, 920–924. [[CrossRef](#)]
61. Kumar, P.; Mathpal, M.C.; Prakash, J.; Hamad, S.; Rao, S.V.; Viljoen, B.C.; Duvenhage, M.-M.; Njoroge, E.G.; Roos, W.D.; Swart, H.C. Study of Tunable Plasmonic, Photoluminescence, and Nonlinear Optical Behavior of Ag Nanoclusters Embedded in a Glass Matrix for Multifunctional Applications. *Phys. Status Solidi* **2019**, *216*, 1800768. [[CrossRef](#)]
62. Manchala, S.; Nagappagari, L.R.; Venkatakrishnan, S.M.; Shanker, V. Solar-Light Harvesting Bimetallic Ag/Au Decorated Graphene Plasmonic System with Efficient Photoelectrochemical Performance for the Enhanced Water Reduction Process. *ACS Appl. Nano Mater.* **2019**, *2*, 4782–4792. [[CrossRef](#)]
63. Fan, B.; Guo, H.; Shi, J.; Shi, C.; Jia, Y.; Wang, H.; Chen, D.; Yang, Y.; Lu, H.; Xu, H.; et al. Facile One-Pot Preparation of Silver/Reduced Graphene Oxide Nanocomposite for Cancer Photodynamic and Photothermal Therapy. *J. Nanosci. Nanotechnol.* **2016**, *16*, 7049–7054. [[CrossRef](#)]
64. Pusty, M.; Rana, A.K.; Kumar, Y.; Sathe, V.; Sen, S.; Shirage, P. Synthesis of Partially Reduced Graphene Oxide/Silver Nanocomposite and Its Inhibitive Action on Pathogenic Fungi Grown Under Ambient Conditions. *ChemistrySelect* **2016**, *1*, 4235–4245. [[CrossRef](#)]
65. Jaworski, S.; Wierzbicki, M.; Sawosz, E.; Jung, A.; Gielerak, G.; Biernat, J.; Jaremek, H.; Łojkowski, W.; Woźniak, B.; Wojnarowicz, J.; et al. Graphene Oxide-Based Nanocomposites Decorated with Silver Nanoparticles as an Antibacterial Agent. *Nanoscale Res. Lett.* **2018**, *13*, 116. [[CrossRef](#)] [[PubMed](#)]
66. Bhunia, S.K.; Jana, N.R. Reduced Graphene Oxide-Silver Nanoparticle Composite as Visible Light Photocatalyst for Degradation of Colorless Endocrine Disruptors. *ACS Appl. Mater. Interfaces* **2014**, *6*, 20085–20092. [[CrossRef](#)] [[PubMed](#)]
67. Ikram, M.; Raza, A.; Imran, M.; Ul-Hamid, A.; Shahbaz, A.; Ali, S. Hydrothermal Synthesis of Silver Decorated Reduced Graphene Oxide (rGO) Nanoflakes with Effective Photocatalytic Activity for Wastewater Treatment. *Nanoscale Res. Lett.* **2020**, *15*, 95. [[CrossRef](#)] [[PubMed](#)]
68. Li, S.; Zhao, J.; Liu, G.; Xu, L.; Tian, Y.; Jiao, A.; Chen, M. Graphene oxide-grafted plasmonic Au@Ag nanoalloys with improved synergistic effects for promoting hot carrier-driven photocatalysis under visible light irradiation. *Nanotechnology* **2020**, *32*, 125401. [[CrossRef](#)] [[PubMed](#)]
69. Li, H.; Zhao, F.; Liu, T.; Zhang, N.; Wang, Y. Design of novel structured Au/g-C₃N₄ nanosheet/reduced graphene oxide nanocomposites for enhanced visible light photocatalytic activities. *Sustain. Energy Fuels* **2020**, *4*, 4086–4095. [[CrossRef](#)]
70. Abd-Elnaem, A.M.; Abd El-Baki, R.F.; Alsaq, F.; Orzechowska, S.; Hamad, D. Composite Nanoarchitectonics of Graphene Oxide for Better Understanding on Structural Effects on Photocatalytic Performance for Methylene Blue Dye. *J. Inorg. Organomet. Polym. Mater.* **2022**, *32*, 1191–1205. [[CrossRef](#)]
71. Mangalam, J.; Kumar, M.; Sharma, M.; Joshi, M. High adsorptivity and visible light assisted photocatalytic activity of silver/reduced graphene oxide (Ag/rGO) nanocomposite for wastewater treatment. *Nano-Struct. Nano-Objects* **2019**, *17*, 58–66. [[CrossRef](#)]
72. Haldorai, Y.; Kim, B.-K.; Jo, Y.-L.; Shim, J.-J. Ag@graphene oxide nanocomposite as an efficient visible-light plasmonic photocatalyst for the degradation of organic pollutants: A facile green synthetic approach. *Mater. Chem. Phys.* **2014**, *143*, 1452–1461. [[CrossRef](#)]
73. Kumar, A.; Sadanandhan, A.M.; Jain, S.L. Silver doped reduced graphene oxide as a promising plasmonic photocatalyst for oxidative coupling of benzylamines under visible light irradiation. *New J. Chem.* **2019**, *43*, 9116–9122. [[CrossRef](#)]
74. Zhang, L.; Du, L.; Yu, X.; Tan, S.; Cai, X.; Yang, P.; Gu, Y.; Mai, W. Significantly Enhanced Photocatalytic Activities and Charge Separation Mechanism of Pd-Decorated ZnO–Graphene Oxide Nanocomposites. *ACS Appl. Mater. Interfaces* **2014**, *6*, 3623–3629. [[CrossRef](#)] [[PubMed](#)]
75. Sarkar, S.; Basak, D. One-step nano-engineering of dispersed Ag–ZnO nanoparticles' hybrid in reduced graphene oxide matrix and its superior photocatalytic property. *CrystEngComm* **2013**, *15*, 7606–7614. [[CrossRef](#)]

76. Gea, S.; Situmorang, S.A.; Pasaribu, N.; Piliang, A.F.R.; Attaurrazaq, B.; Sari, R.M.; Pasaribu, K.M.; Goutianos, S. Facile synthesis of ZnO–Ag nanocomposite supported by graphene oxide with stabilised band-gap and wider visible-light region for photocatalyst application. *J. Mater. Res. Technol.* **2022**, *19*, 2730–2741. [[CrossRef](#)]
77. Chen, Q.; Yu, Z.; Li, F.; Yang, Y.; Pan, Y.; Peng, Y.; Yang, X.; Zeng, G. A novel photocatalytic membrane decorated with RGO-Ag-TiO₂ for dye degradation and oil–water emulsion separation. *J. Chem. Technol. Biotechnol.* **2018**, *93*, 761–775. [[CrossRef](#)]
78. Zhang, X.; Wang, N.; Liu, R.; Wang, X.; Zhu, Y.; Zhang, J. SERS and the photo-catalytic performance of Ag/TiO₂/graphene composites. *Opt. Mater. Express* **2018**, *8*, 704–717. [[CrossRef](#)]
79. Qi, H.-P.; Wang, H.-L.; Zhao, D.-Y.; Jiang, W.-F. Preparation and photocatalytic activity of Ag-modified GO-TiO₂ mesocrystals under visible light irradiation. *Appl. Surf. Sci.* **2019**, *480*, 105–1144. [[CrossRef](#)]
80. Wang, Y.; Zhang, M.; Yu, H.; Zuo, Y.; Gao, J.; He, G.; Sun, Z. Facile fabrication of Ag/graphene oxide/TiO₂ nanorod array as a powerful substrate for photocatalytic degradation and surface-enhanced Raman scattering detection. *Appl. Catal. B Environ.* **2019**, *252*, 174–186. [[CrossRef](#)]
81. Leong, K.H.; Sim, L.C.; Bahnemann, D.; Jang, M.; Ibrahim, S.; Saravanan, P. Reduced graphene oxide and Ag wrapped TiO₂ photocatalyst for enhanced visible light photocatalysis. *APL Mater.* **2015**, *3*, 104503. [[CrossRef](#)]
82. Kisielewska, A.; Spilarewicz-Stanek, K.; Cichomski, M.; Kozłowski, W.; Piwoński, I. The role of graphene oxide and its reduced form in the in situ photocatalytic growth of silver nanoparticles on graphene-TiO₂ nanocomposites. *Appl. Surf. Sci.* **2022**, *576*, 151759. [[CrossRef](#)]
83. Krishnamoorthy, K.; Mohan, R.; Kim, S.-J. Graphene oxide as a photocatalytic material. *Appl. Phys. Lett.* **2011**, *98*, 244101. [[CrossRef](#)]
84. Siong, V.L.E.; Tai, X.H.; Lee, K.M.; Juan, J.C.; Lai, C.W. Unveiling the enhanced photoelectrochemical and photocatalytic properties of reduced graphene oxide for photodegradation of methylene blue dye. *RSC Adv.* **2020**, *10*, 37905–37915. [[CrossRef](#)]
85. Siong, V.L.E.; Lee, K.M.; Juan, J.C.; Lai, C.W.; Tai, X.H.; Khe, C.S. Removal of methylene blue dye by solvothermally reduced graphene oxide: A metal-free adsorption and photodegradation method. *RSC Adv.* **2019**, *9*, 37686–37695. [[CrossRef](#)] [[PubMed](#)]
86. Matsumoto, Y.; Koinuma, M.; Ida, S.; Hayami, S.; Taniguchi, T.; Hatakeyama, K.; Tateishi, H.; Watanabe, Y.; Amano, S. Photoreaction of Graphene Oxide Nanosheets in Water. *J. Phys. Chem. C* **2011**, *115*, 19280–19286. [[CrossRef](#)]
87. Singh, M.; Bajaj, N.K.; Bhardwaj, A.; Singh, P.; Kumar, P.; Sharma, J. Study of photocatalytic and antibacterial activities of graphene oxide nanosheets. *Adv. Compos. Hybrid Mater.* **2018**, *1*, 759–765. [[CrossRef](#)]
88. Wong, C.P.P.; Lai, C.W.; Lee, K.M.; Hamid, S.B.A. Advanced Chemical Reduction of Reduced Graphene Oxide and Its Photocatalytic Activity in Degrading Reactive Black 5. *Materials* **2015**, *8*, 7118–7128. [[CrossRef](#)]
89. Moussa, H.; Giroto, E.; Mozet, K.; Alem, H.; Medjahdi, G.; Schneider, R. ZnO rods/reduced graphene oxide composites prepared via a solvothermal reaction for efficient sunlight-driven photocatalysis. *Appl. Catal. B Environ.* **2016**, *185*, 11–21. [[CrossRef](#)]
90. Xue, B.; Zou, Y. High photocatalytic activity of ZnO–graphene composite. *J. Colloid Interface Sci.* **2018**, *529*, 306–313. [[CrossRef](#)]
91. Singh, M.; Kaushal, S.; Singh, P.; Sharma, J. Boron doped graphene oxide with enhanced photocatalytic activity for organic pollutants. *J. Photochem. Photobiol. A Chem.* **2018**, *364*, 130–139. [[CrossRef](#)]
92. Junaid, M.; Khir, M.H.M.; Witjaksono, G.; Tansu, N.; Saheed, M.S.M.; Kumar, P.; Ullah, Z.; Yar, A.; Usman, F. Boron-Doped Reduced Graphene Oxide with Tunable Bandgap and Enhanced Surface Plasmon Resonance. *Molecules* **2020**, *25*, 3646. [[CrossRef](#)] [[PubMed](#)]
93. Tang, Z.-R.; Zhang, Y.; Zhang, N.; Xu, Y.-J. New insight into the enhanced visible light photocatalytic activity over boron-doped reduced graphene oxide. *Nanoscale* **2015**, *7*, 7030–7034. [[CrossRef](#)] [[PubMed](#)]
94. Tai, X.H.; Lai, C.W.; Yang, T.C.K.; Chen, C.-Y.; Abdullah, A.H.; Lee, K.M.; Juan, J.C. Effective oxygenated boron groups of boron-doped photoreduced graphene oxide for photocatalytic removal of volatile organic compounds. *J. Environ. Chem. Eng.* **2022**, *10*, 108047. [[CrossRef](#)]